JOURNAL OF MATERIALS SCIENCE 22 (1987) 2816–2822

Low-thermal expansion polycrystalline tantalum tungstate ceramics

J. Z. WU
North-Western Institute of Light Industry, China
T. OTA, I. YAMAI
Ceramic Engineering Research Laboratory, Nagoya Institute of Technology, Japan

The synthesis of thermal-shock-resistant materials from the system Ta_2O_5–WO_3 was investigated. Ta_2WO_8 had a very low unit-cell thermal expansion coefficient ($+0.5 \times 10^{-6}\,°C^{-1}$). $Ta_{30}W_2O_{81}$ also had a relatively low coefficient ($+4.0 \times 10^{-6}\,°C^{-1}$) and a thermal durability over 1600° C. The thermal expansion curves of these polycrystalline ceramics were lowered because of microcracks caused by the large thermal expansion anisotropy of the crystal axes and were accompanied by hysteresis loops. The densification of Ta_2WO_8 ceramic was promoted by the addition of some metal oxides, and the strong ceramic of $Ta_{30}W_2O_{81}$ was obtained by controlling grain growth.

1. Introduction

Polycrystalline spodumene and cordierite ceramics are used as thermal-shock-resistant materials. Aluminium titanate is also utilized for this purpose. Spodumen and cordierite crystals have low unit-cell thermal expansion coefficients resulting from three-dimensional averaging of the thermal expansion coefficient of their three crystal axes. The unit cell of aluminium titanate, however, has a higher average thermal expansion coefficient; nevertheless, low thermal expansion is responsible for microcrack formation in the polycrystalline ceramics. These microcracks are caused by the large thermal expansion anisotropy of the crystal axes.

A study to identify low-expansion oxides which may have more excellent thermal-shock resistance led to several promising materials, some of which existed in the system Ta_2O_5–WO_3 [1]. The low-to-negative thermal expansion and the expansion hysteresis with minimal observable microcracking of tantalum tungstates ($Ta_{22}W_4O_{67}$, Ta_2WO_8 and $Ta_{16}W_{18}O_{94}$) have been reported by Holcombe and Smith [2]. More detailed studies have not yet been conducted. In the present study, the thermal expansion of their crystal lattices was determined. From these the thermal expansion behaviour of their polycrystalline ceramics were discussed, and the synthesis of tantalum tungstate ceramics as thermal-shock-resistant materials was investigated.

2. Experimental procedure

Starting materials were reagent grade tantalum pentoxide (Ta_2O_5 = 99.8%, WAKO pure chemical industries Ltd) and tungsten trioxide (WO_3). Each of the Ta_2O_5–WO_3 compounds was prepared as follows: a given molar ratio (4 : 9, 1 : 1, 11 : 4, 15 : 2) of Ta_2O_5 and WO_3 was mixed, and calcined at 1200° C for 4 to 16 h. The powders $Ta_{16}W_{18}O_{94}$, Ta_2WO_8, $Ta_{22}W_4O_{67}$ and $Ta_{30}W_2O_{81}$ thus obtained were gound to a 1 μm grain size, and 0.2 to 5 wt % of various metal oxides were added as a sintering aid. Test specimens were then formed under 50 to 150 MPa in the shape of 16 mm diameter tablets and/or 5 mm × 50 mm × 5 mm bars. The tablets and/or bars were then sintered at temperatures ranging from 1100 to 1600° C. The bulk density was determined by measuring the weight and size of a sintered specimen.

Thermal expansion of the sintered tantalum tungstate ceramics was measured with a fused-silica or alumina dilatometer at a heating rate of $10°\,C\,min^{-1}$ from room temperature to 1000° C. When the thermal expansion–temperature curves showed hysteresis loops between the heating and cooling, each measurement was performed at least twice more to ensure that the loops were the same for each sample. The lattice thermal expansions of tantalum tungstates were determined by high-temperature X-ray diffraction measurements up to 1000° C. Procedures for measurement and data processing have been described previously in detail [3].

The fracture surfaces of these sintered ceramics were observed with a scanning electron microscope.

3. Results and discussion

3.1. Thermal expansion of tantalum tungstate crystal lattice

Fig. 1 shows the thermal expansion of the crystal axes of tantalum tungstates. All these crystals showed anisotropic thermal expansion behaviour, therefore it could be deduced that the low thermal expansion curves exhibiting hysteresis loops reported by Holcombe and Smith [2] were due to the microcracks caused by the large thermal expansion anisotropy of the crystal axes. Within the range of room temperature to 1000° C, and a and b axes expanded continuously with increasing temperature, while the c axis contracted. The calculated average linear thermal expansion coefficients

0022–2461/87 $03.00 + .12

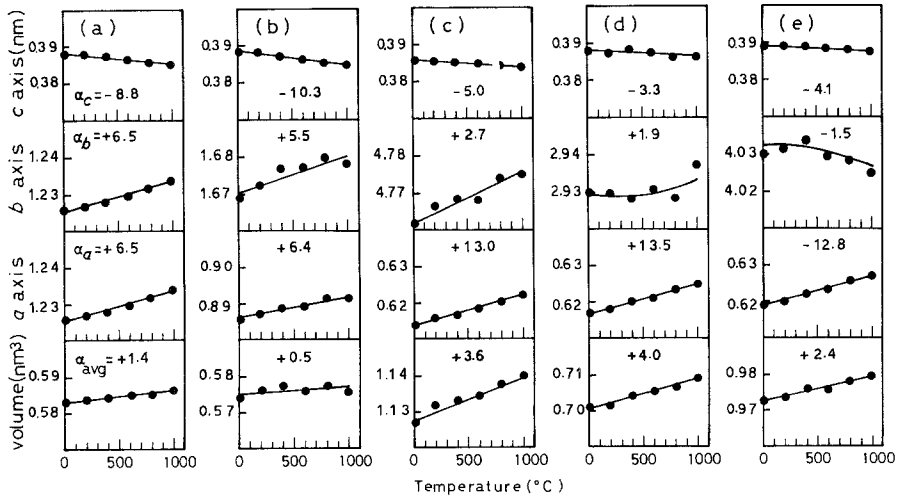

Figure 1 Changes in lattice constants at elevated temperatures. (a) $Ta_{16}W_{18}O_{94}$, (b) Ta_2WO_8 (c) $Ta_{22}W_4O_{67}$, (d) $Ta_{30}W_2O_{81}$, (e) Ta_2O_5, ($\times 10^{-6}\,°C^{-1}$ as a unit of CTE).

(CTE) of the unit cells were low: CTE of $Ta_{16}W_{18}O_{94}$, Ta_2WO_8, $Ta_{22}W_4O_{67}$ and $Ta_{30}W_2O_{81}$ were $+1.4 \times 10^{-6}\,°C^{-1}$, $+0.5 \times 10^{-6}\,°C^{-1}$, $+3.6 \times 10^{-6}\,°C^{-1}$ and $+4.0 \times 10^{-6}\,°C^{-1}$, respectively. In particular, the CTE of the unit cell of Ta_2WO_8 was near zero and close to that of quartz glass. This means that the Ta_2WO_8 ceramic will exhibit a low thermal expansion even if no microcracks form in the polycrystalline ceramic. Consequently, Ta_2WO_8 appeared to be the most suitable for an ultra-low thermal expansion material in the system Ta_2O_5–WO_3.

$Ta_{16}W_{18}O_{94}$ (a) and Ta_2WO_8 (b) are members of a family with formulae such as $mTa_2O_5 \cdot nWO_3$ in the tungsten bronze structure, consisting of a column of pentagonal bipyramidal coordination groups sharing edges with the surrounding columns of octahedra; these multiple columns then form the three-dimensional framework by corner-sharing [4–8]. The structures of $Ta_{22}W_4O_{67}$ (c) and $Ta_{30}W_2O_{81}$ (d) are of the same general type as L-Ta_2O_5 (e), consisting of chains built from octahedral or pentagonal bipyramidal groups sharing two opposite vertices, these chains being joined by corner or edge-sharing to give the three-dimensional structure [4, 5, 9, 10]. Consequently, in the characteristics of the thermal expansion of these crystals, as shown in Fig. 1, there is some analogy between (a) and (b), as well as between (c), (d) and (e). On the whole, the thermal expansion coefficients of the *a* and *b* axes, which are parallel to the sheet of polyhedra joined by edge-sharing within the (0 0 1) plane, are positive; and the coefficient of the *c*-axis, which is perpendicular to the sheet, i.e., along the direction connected by corner-sharing, is negative. Therefore, it can be presumed that extension or distortion of the structure along [0 0 1] which occurred by corner-sharing is responsible for the negative expansion.

3.2. Thermal durability

The phase equilibrium diagram of the system Ta_2O_5–WO_3 has been reported by Roth *et al.* [10]. Ta_2WO_8 and $Ta_{22}W_4O_{67}$ melt incongruently at 1580 and 1605° C, respectively. $Ta_{30}W_2O_{81}$ is the most stable composition, having a congruent melting point at 1815° C. These data are different from those of Holcombe [1]. The data from the present study are plotted as black (stable) and white (decomposed) marks in the phase diagram (Fig. 2). $Ta_{16}W_{18}O_{94}$ decomposed into $Ta_{30}W_2O_{81}$ and Ta_2WO_8, and Ta_2WO_8 was partially decomposed into $Ta_{30}W_2O_{81}$ by calcining at 1400° C for 24 h, where the weight loss was 40 and 18%, respectively. $Ta_{22}W_4O_{67}$ and $Ta_{30}W_2O_{81}$ are stabilized phases similar in structure to the low-temperature polymorph of Ta_2O_5 (L-Ta_2O_5), which transforms to a high-temperature form (H-Ta_2O_5) at 1360° C [10]. $Ta_{30}W_2O_{81}$ was stable up to 1600° C and its weight loss was as little as 0.15% at 1400° C over 24 h and 0.5% at 1600° C over 2 h. Thus, because of its overall lower rate of volatilization and stability, $Ta_{30}W_2O_{81}$ was expected to be the thermal-shock-resistant material used at a higher temperature than the other compounds in the system Ta_2O_5–WO_3.

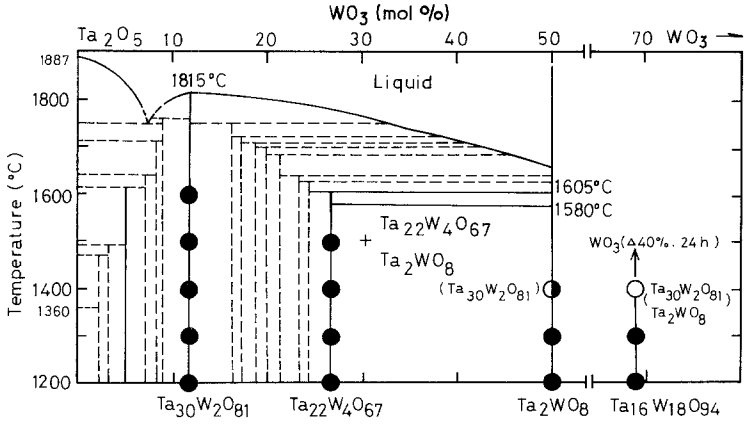

Figure 2 Phase diagram of the system Ta_2O_5–Ta_2WO_8.

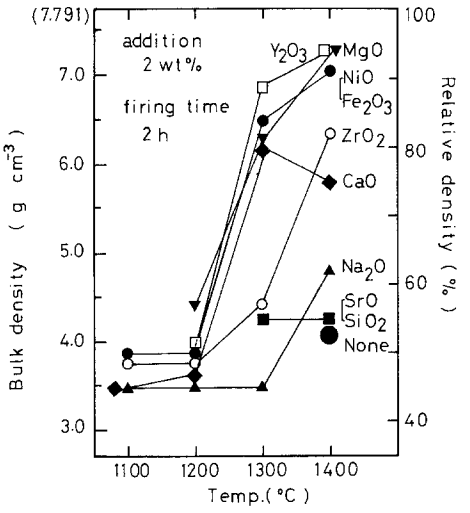

Figure 3 Densification curves for compact Ta_2WO_8 sintered with additives.

3.3. Preparation of Ta_2WO_8 ceramic

Dense polycrystalline Ta_2WO_8 ceramic could not be obtained by firing pure Ta_2WO_8 even at 1400° C for 2 h. Accordingly, various metal oxides were examined in order to find a sintering aid for obtaining dense ceramics at lower temperatures. Several metal oxides were effective for densification of the polycrystalline ceramic as shown in Fig. 3. In the case of adding MgO, Y_2O_3, NiO etc., the density achieved was over 90% theoretical. Fig. 4 shows the typical microstructures. Specimens sintered with MgO or CaO partially melted, and resulted in the exaggerated grain growth at a higher temperature. On the other hand, specimens sintered with NiO or Y_2O_3 consisted of relatively fine grains.

Fig. 5 shows the densification curves and the strength of compacts sintered with 1 wt % Y_2O_3. As the firing time was longer, the density was higher. On the other hand, the strength increased initially, then reached a maximum at 60 min, and decreased. Longer firing resulted in grain growth and corresponding microcracking, as shown clearly in Figs 4g to i. Therefore, it was evident that microcracking was responsible for the lowered strength. Microcracking is related to grain size, and occurs at a certain grain size [11–13]. As the grain size of a polycrystalline ceramic is larger, more microcracks occur, resulting in lowering of the strength. Microcracks also have an influence on thermal expansion; the very low thermal expansion with hysteresis is attributed to the occurrence and healing of internal microcracks [14]. Fig. 6 shows the typical thermal expansion curves. The specimen containing not only larger grains but also fine grains exhibited lower thermal expansion than the average thermal expansion expected from the unit cell, and

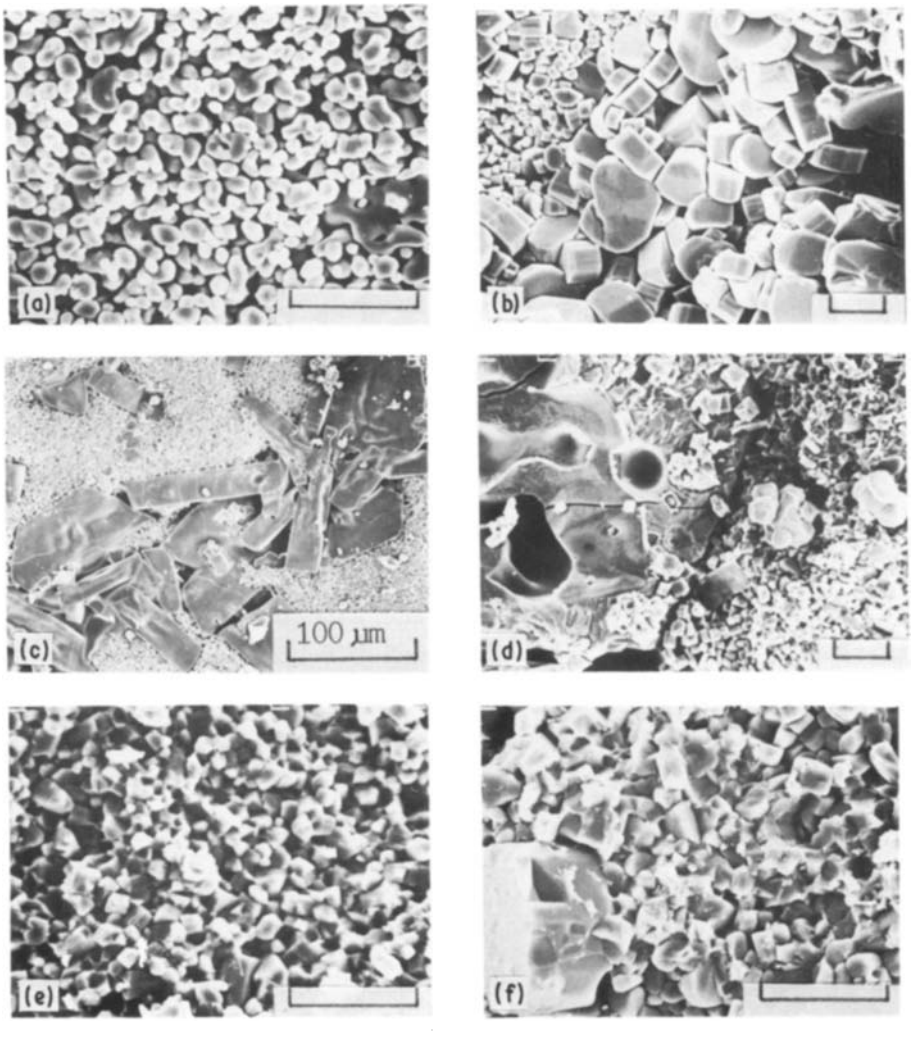

Figure 4 Scanning electron micrographs of fracture surfaces of Ta_2WO_8 ceramics sintered with (a) no additives, (b) 2 wt % MgO, (c) 2 wt % MgO (surface), (d) 2 wt % CaO, (e) 2 wt % NiO, (f) 2 wt % Y_2O_3 for 2 h, (g) 1 wt % Y_2O_3 for 15 min, (h) 60 min, and (i) 120 min at 1400° C (bar = 10 μm).

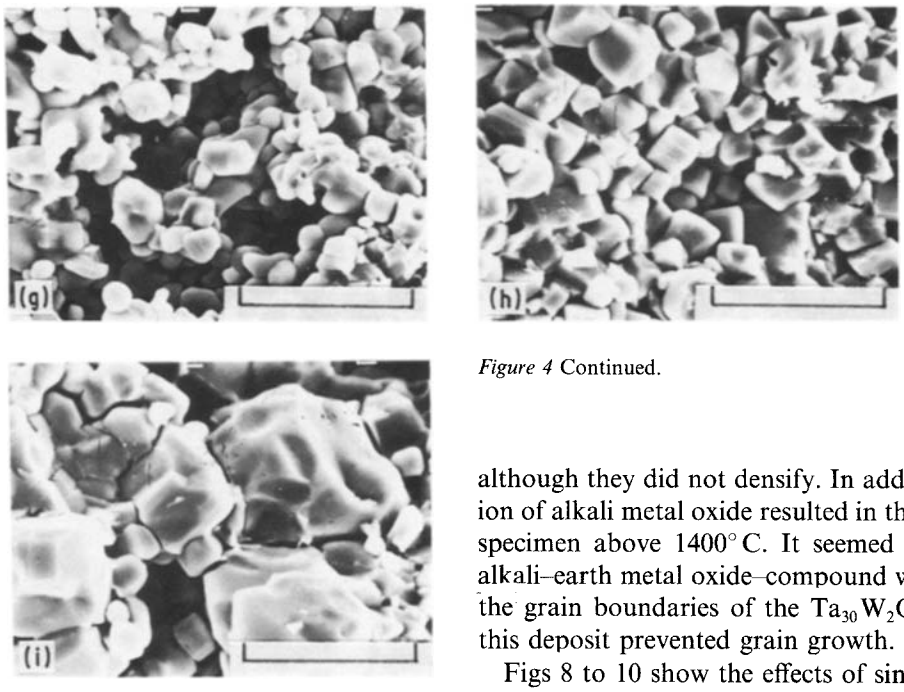

Figure 4 Continued.

had a hysteresis loop. Consequently, it was thought that microcracking began at very fine grains. This seemed to be caused by the very large thermal expansion anisotropy ($\Delta\alpha_{max} = +15.2 \times 10^{-6}\,°C^{-1}$, where $\Delta\alpha_{max}$ is the maximum difference in single-crystal thermal expansion coefficients of the crystal axes).

3.4. Preparation of $Ta_{30}W_2O_{81}$ ceramic

A polycrystalline $Ta_{30}W_2O_{81}$ ceramic densified over 95% by firing pure $Ta_{30}W_2O_{81}$ at > 1400° C. However, grains grew abruptly and grain-boundary cracking occurred as shown in Fig. 7a. It was thought that this resulted from the large thermal expansion anisotropy ($\Delta\alpha_{max} = 16.9 \times 10^{-6}\,°C^{-1}$) of the $Ta_{30}W_2O_{81}$ crystal axes. Whenever these grain-boundary cracks connect, a crack network resulted so that the sintered ceramic broke into a powder with little force. Therefore, it was essential to the polycrystalline $Ta_{30}W_2O_{81}$ ceramic that grain growth was controlled in order to increase its strength. For this purpose, various metal oxides were examined to find a grain growth depressor. As shown in Fig. 7, the specimen sintered with alkali and alkali–earth metal oxides consisted of fine grains, although they did not densify. In addition, the addition of alkali metal oxide resulted in the melting of the specimen above 1400° C. It seemed that alkali and alkali–earth metal oxide–compound was deposited at the grain boundaries of the $Ta_{30}W_2O_{81}$ ceramic and this deposit prevented grain growth.

Figs 8 to 10 show the effects of sintering time and the amount of additive on grain size in the $Ta_{30}W_2O_{81}$ ceramic sintered with alkali–earth metal oxide. Grains grew rapidly with firing time, resulting in a slight lowering of the relative density as well as a lowering of the thermal expansion due to microcracking. The grain size decreased with increasing amount of SrO, and the thermal expansion coefficient increased. 5 wt % SrO seemed to be sufficient to depress grain growth. However, densification was also depressed on addition of relatively large amounts of alkali-earth metal oxide such as 5 wt % SrO sintered at 1500° C, so that these specimens were all weak in strength.

In order to obtain a dense and strong ceramic, a transition metal oxide (such as NiO), which promoted slight densification, was added together with an alkali–earth metal oxide (such as SrO) as a depressor of grain growth. Figs 11 and 12 show the strength and the microstructure in the case of additions of both SrO and NiO. The specimen densified up to 82% by sintering with 5 wt % SrO and 1 wt % NiO at 1600° C for 2 h, and exhibited a dense microstructure, such that the bending strength was improved up to 50 MPa.

Fig. 13 shows the typical thermal expansion curves. The specimen including clear microcracks exhibited a low thermal expansion curve with a hysteresis loop.

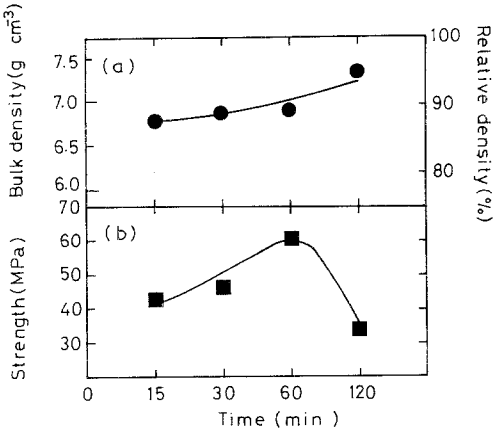

Figure 5 Relationship of densification (a) and strength (b) to sintering time for compact Ta_2WO_8 with addition of 1 wt % Y_2O_3 at 1400° C.

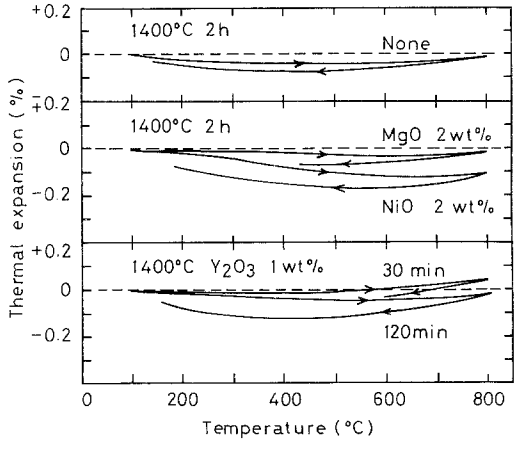

Figure 6 Thermal expansion curves for tantalum tungstate ceramics Ta_2WO_8.

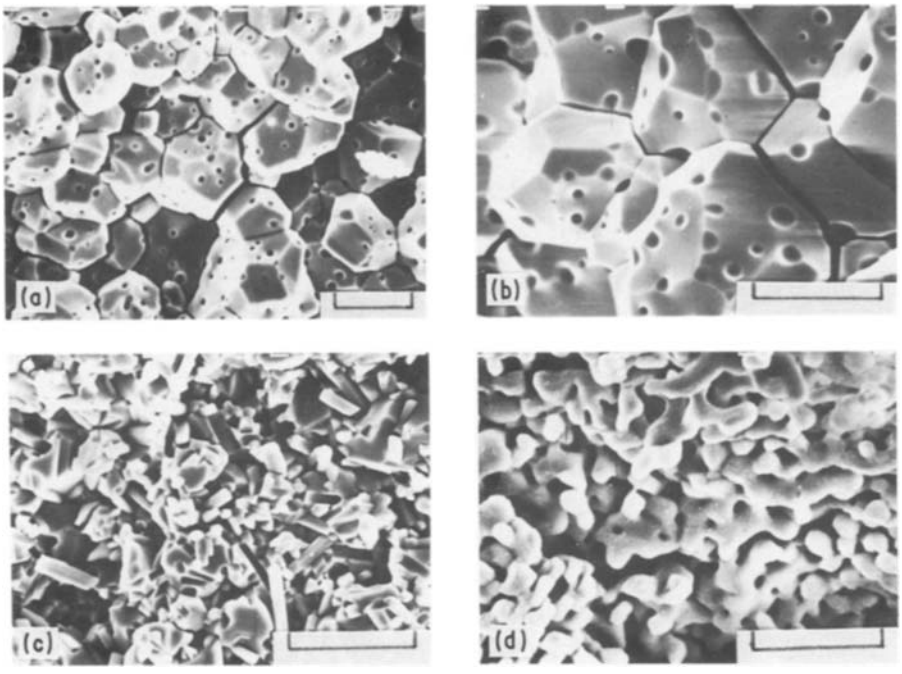

Figure 7 Scanning electron micrographs of fracture surfaces of $Ta_{30}W_2O_{81}$ ceramics sintered for 2 h (a) at 1400° C, (b) with 2 wt % NiO at 1400° C, (c) with 2 wt % BaO at 1500° C, and (d) with 2 wt % Li_2O at 1400° C (bar = 10 μm).

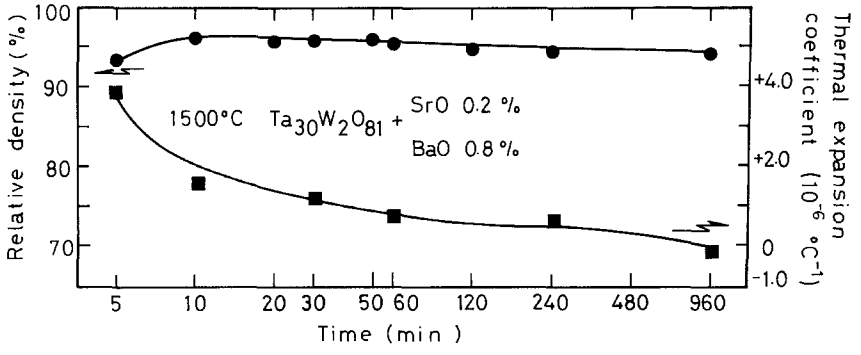

Figure 8 Variation of densification and thermal expansion with sintering time for compact $Ta_{30}W_2O_{81}$.

On the other hand, the thermal expansion of the specimen with controlled grain growth approached the average thermal expansion of the unit cell, and showed almost no hysteresis.

4. Conclusion

In the present study, it was clear that excellent thermal-shock-resistance materials existed in the system Ta_2O_5–WO_3. Ta_2WO_8 had a very low thermal expansion coefficient of the unit cell, $+0.5 \times 10^{-6}\,°C^{-1}$, close to that of quartz glass. Densification of the Ta_2WO_8 ceramic was promoted by adding a metal oxide such as NiO and Y_2O_3. Ta_2WO_8 ceramic sintered with addition of 1 wt % Y_2O_3 at 1400° C for 1 h had a relative density of about 90%, a low thermal expansion coefficient of $+0.3 \times 10^{-6}\,°C^{-1}$ and the highest bending strength of 60 MPa. In addition, because of decomposition and exaggerated grain growth at higher temperatures, Ta_2WO_8 ceramic is suitable as an ultra low thermal expansion material below 1400° C.

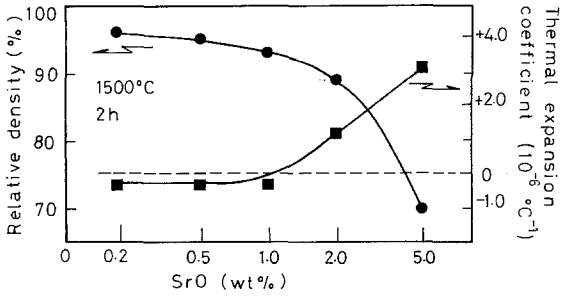

Figure 9 Variation of densification and thermal expansion with addition amount for compact $Ta_{30}W_2O_{81}$.

$Ta_{30}W_2O_{81}$ had a relatively low thermal expansion coefficient of the unit cell, $+4.0 \times 10^{-6}\,°C^{-1}$, and a higher thermal durability over 1600° C. Although $Ta_{30}W_2O_{81}$ densified over 95% by firing at 1400° C, cracking resulting from the large thermal expansion anisotropy of crystal axes could not be avoided. Consequently, the strong ceramic of $Ta_{30}W_2O_{81}$ was obtained by controlling grain growth by the addition of alkali–earth metal oxide and transition metal oxide. $Ta_{30}W_2O_{81}$ ceramic sintered with the addition of 5 wt % SrO as a depressor of grain growth and 1 wt % NiO as a promoter of densification at 1600° C for 2 h, had a relative density of 82%, a low thermal expansion coefficient of $+3.0 \times 10^{-6}\,°C^{-1}$, and a bending strength of 50 MPa.

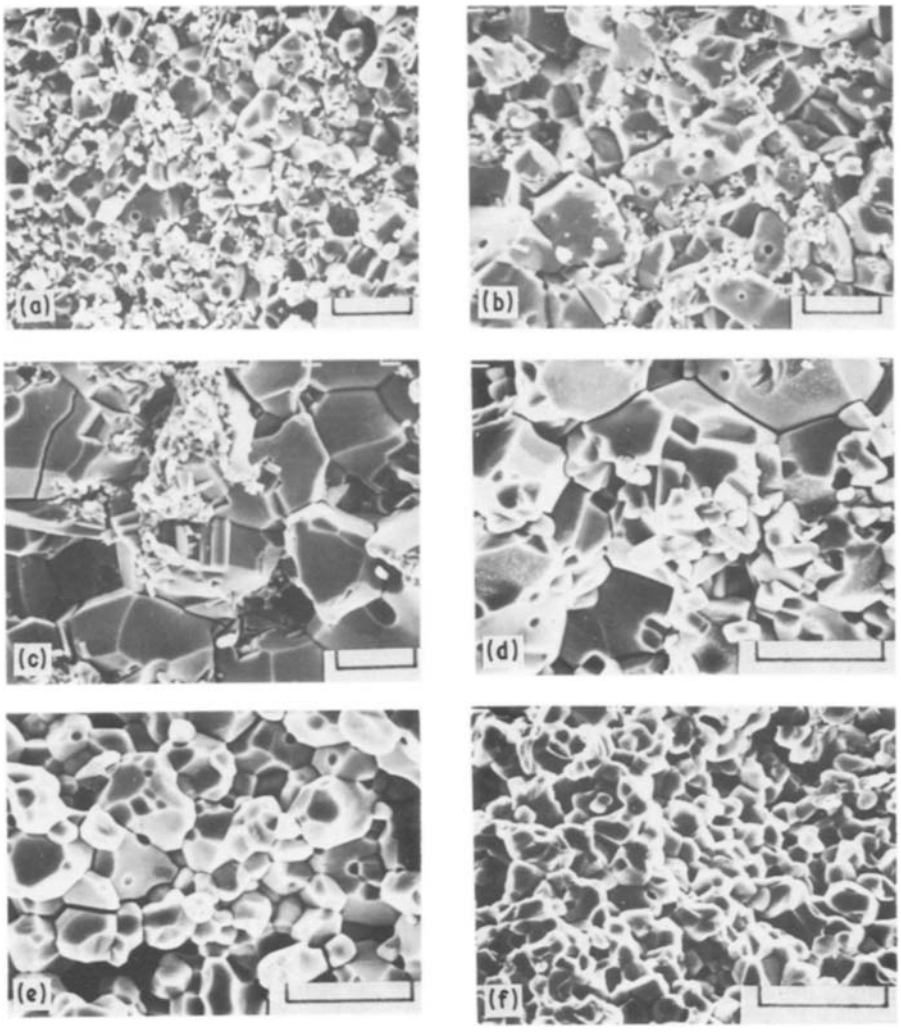

Figure 10 Scanning electron micrograph of fracture surface of $Ta_{30}W_2O_{81}$ sintered at 1500° C (a) with 0.2 wt % SrO and 0.8 wt % BaO for 5 min, (b) 10 min, (c) 16 h, (d) for 2 h with 1 wt %, (e) 2 wt %, and (f) 5 wt % SrO (bar = 10 μm).

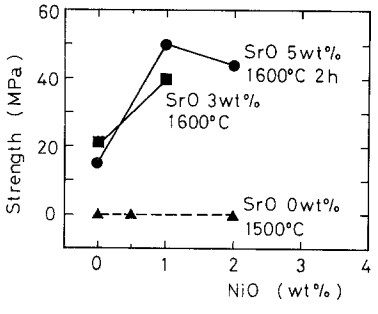

Figure 11 Variation of strength with addition of NiO and SrO.

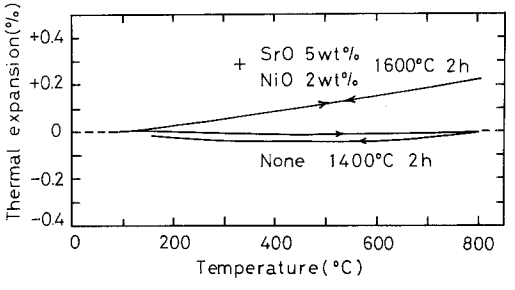

Figure 13 Thermal expansion curves for tantalum tungstate $Ta_{30}W_2O_{81}$ sintered for 2 h.

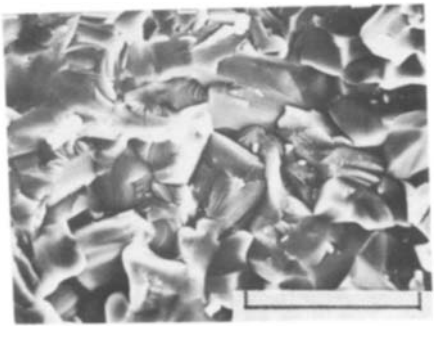

Figure 12 Scanning electron micrograph of fracture surface of $Ta_{30}W_2O_{81}$ ceramics sintered at 1600° C for 2 h with 5 wt % SrO and 1 wt % NiO (bar = 10 μm).

References

1. C. E. HOLCOMBE Jr, *Bull. Amer. Ceram.* **59** (1980) 1219.
2. C. E. HOLCOMBE Jr and D. D. SMITH, *J. Amer. Ceram. Soc.* **61** (1978) 163.
3. T. OOTA and I. YAMAI, *ibid.* **69** (1986) 1.
4. A. F. WELLS, "Structural Inorganic Chemistry" (Clarendon Press, Oxford, 1975) pp. 454, 508.
5. R. S. ROTH and J. L. WARING, *J. Res. Natl Bur. Stand.* **70A** (1966) 281.
6. A. W. SLEIGHT, *Acta Chem. Scand.* **20** (1966) 1102.
7. M. LUNDRERG, *ibid.* **26** (1972) 2932.
8. A. SANTORO, R. S. ROTH and D. MINOR, *Acta Crystallogr.* **B35** (1979) 1202.
9. N. C. STEPHENSON and R. S. ROTH, *ibid.* **B27** (1971) 1010.

10. R. S. ROTH, J. L. WARING and H. S. PARKER, *J. Solid State Chem.* **2** (1970) 445.
11. J. A. KUSZYK and R. C. BRADT, *J. Amer. Ceram. Soc.* **56** (1973) 420.
12. J. J. CLEVELAND and R. C. BRADT, *ibid.* **61** (1978) 478.
13. R. W. RICE and R. C. POHANKA, *ibid.* **62** (1979) 559.
14. E. A. BUSH and F. A. HUMMEL, *ibid.* **41** (1958) 189.

Received 8 September
and accepted 12 November 1986